ON THE EFFECTS OF WINDOWING ON THE DISCRETIZATION OF THE FRACTIONAL FOURIER TRANSFORM

Balu Santhanam, Thalanayar S Santhanam, and Satish Mandal

Department of ECE, University of New Mexico
Albuquerque, NM: 87131, Email: bsanthan@unm.edu

ABSTRACT

The eigenvalue degeneracy problem inherent in the *discrete Fourier transform* (DFT) matrix operator and the development of a full basis of orthogonal eigenvectors have been addressed via a commuting matrix, devoid of the aforementioned eigenvalue degeneracy problem, that also serves as a discrete version of the Gauss-Hermite (G-H) differential operator.

This G-H operator is however, is not bandlimited, and existing discretization efforts run into distortion problems that manifest as deviation from the ideal linear eigenvalue spectrum, aliasing in the eigenvectors, and as a non-invertible peak to parameter mapping associated with the discretization restricting its ability to uniquely represent multicomponent chirp signals. Existing approaches do not account for the effects of windowing on discretization.

In this paper, we focus on distortion issues associated with the discretization of the G-H operator and their sources. We specifically analyze the discrete version of the G-H operator based on quantum mechanics in finite dimensions (QMFD), by computing its underlying peak to parameter mapping and its invertibility to subsequently present a representation of the operator with improved mapping invertibility via use of suitable windowing of the eigenvalue spectrum.

Keywords: discrete Fourier transform, eigenvectors, discrete Fractional Fourier transform, aliasing, peak to parameter mapping, quantum mechanics in finite dimensions, windowing.

1. DISTORTION SOURCES

In recent years, the *fractional Fourier transform* (FRFT) has become a very useful tool for time-frequency analysis for signals with modulation [2]. The kernel of the continuous-time FRFT [2] is given by:

$$K_\alpha(t,u) = \sqrt{\frac{1-j\cot\alpha}{2\pi}}\exp\left(j(t^2+u^2)\cot\alpha/2 - jtu\csc\alpha\right)$$

The corresponding Mehler's expansion for the chirped kernel is:

$$K_\alpha(t,u) = \sum_{k=0}^{\infty}\exp\left(-jk\alpha\right)h_k(t)h_k(u), \tag{1}$$

where $h_k(t)$ denoted the k-th Gauss-Hermite (G-H) function. This chirped kernel produces a Dirac impulse for the FRFT, when the input signal is a chirp signal with a specified center-frequency ω_o and chirp rate c_r for a specific angle α_o:

$$\begin{aligned} X_{\alpha_o}(u) &= \exp\left(j\frac{\cot\alpha_o}{2}u^2\right)\sqrt{\frac{1-j\cot\alpha_o}{2\pi}} \\ &\times \quad 2\pi\delta(\omega_o - u\csc\alpha_o) \text{ for } \alpha_o = \cot^{-1}(-2c_r). \end{aligned}$$

This chirped kernel of the FRFT is however, not bandlimited, and causes distortion in discrete versions of the FRFT.
Existing commuting methods for computing the discrete version of the FRFT (DFRFT) [4, 5, 3] use a eigenvalue decomposition of the form:

$$\mathbf{A}_\alpha(\mathbf{x}) = \mathbf{V}\mathbf{\Lambda}^{\frac{2\alpha}{\pi}}\mathbf{V}^T\mathbf{x} = \sum_{k=0}^{N-1}\exp(-jk\alpha)\mathbf{v}_k\mathbf{v}_k^T\mathbf{x}, \tag{2}$$

where $\mathbf{V}$ is a fully orthogonal basis of DFT or CDFT eigenvectors, obtained from a commuting matrix, that serve as discrete counterparts of the G-H functions. As seen in earlier work [8], the effects of discretization results in a non-invertible peak to parameter mapping restricting the capabilities of the DFrFT.

2. SOURCES OF DISRETISATION ERRORS

From Eq. (1) and Eq. (2), we can observe that in the transition from the continuous to the discrete FRFT, there are two phenomena happening:

1. Truncation or windowing of the IIR eigenvalue sequence of the G-H operator with a rectangular window of duration N samples:
$$\lambda_w[k] = \exp(-jk\alpha)w[k],$$
where $w[n]$ is the N-point boxcar window [1]. This is analogous to the window based FIR filter design technique, where a IIR impulse response is approximated with an FIR windowed equivalent or spectral analysis using the DFT. This will result in spectral distortion of the eigenvalue sequence:
$$\Lambda_w(e^{j\omega}) = W(e^{j(\omega-\alpha)}),$$
where $W(e^{j\omega})$ denotes the DTFT of the window function [1] used. The boxcar window produces the narrowest main lobe but has the smallest main lobe to sidelobe spectral amplitude ratio, thereby producing more sidelobes in the DTFT of the windowed eigenvalue sequence. Existing approaches towards G-H operator discretization, however, do not accommodate windowing effects.

This research was supported by the United States Department of Energy (Award DE-NA 0002494) and the National Nuclear Security Administration (NA-221)

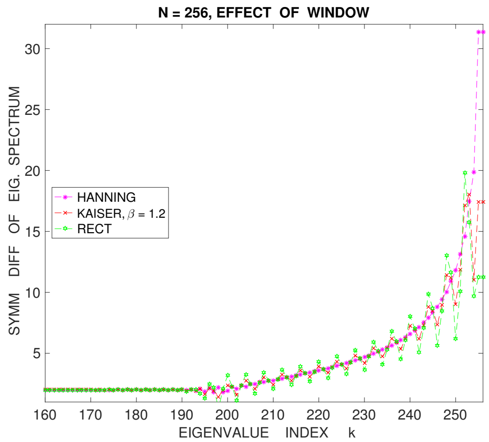

Fig. 1. Effect of windowing on the eigenvalue spectrum: symmetric difference of the eigenvalue spectrum of the commuting matrix using different windows on the diagonal matrix $\mathbf{Q}^2$. Windowing using an appropriate data window reduces the deviation from a linear eigenvalue spectrum at the tail-end of the eigenvalue spectrum.

2. Discretization or sampling of the G-H functions to yield DFT/CDFT eigenvectors which will in turn result in spectral aliasing in the eigenvectors corresponding to the higher G-H modes with frequency content at the edges of $|\omega| < \pi$:

$$V_k(e^{j\omega}) = \frac{1}{T_s}\sum_{k=-\infty}^{\infty} H_k\left(\frac{\omega - 2k\pi}{T_s}\right), \quad |w| < \pi,$$

where T_s is the sampling period associated with the discretization of the G-H functions.

Several commuting matrix approaches towards furnishing the unitary basis of DFT/CDFT eigenvectors have been studied [4, 5, 3] staking the claim that they are discrete versions of the G-H operator.

In this paper, we focus on the distortion issues identified above, that arise in the G-H operator discretization and in particular, incorporate windowing effects into the QMFD approach [3]. We further investigate extensions of the QMFD approach [3, 7], in light of these sources, that result in a commuting matrix and associated eigenvectors with a reduced degree of distortion. We further show through simulation results that a suitable choice of window applied to the eigenvalue sequence of the discrete operator results in improvement of the invertibility of the underlying peak to parameter mapping and to the associated mean squared errors of chirp parameter estimates that are of importance in SAR vibrometry applications [9, 10].

3. QMFD APPROACH: DIAGONAL Q AND QUASI-TOEPLITZ MATRICES

We first focus our attention on the QMFD approach in [3, 7]:

$$\begin{aligned}\mathbf{Q} &= \sqrt{\frac{2\pi}{N}}\mathrm{diag}\,(-m,\ldots,m) \\ \mathbf{P} &= \mathbf{WQW}^H \\ \mathbf{T} &= \mathbf{P}^2 + \mathbf{Q}^2,\end{aligned} \qquad (3)$$

where $\mathbf{Q}$ and $\mathbf{P}$ denote the finite dimensional position and momentum operators and $\mathbf{W}$ denotes the centered version of the DFT:

$$\mathbf{W}_{rs} = \frac{1}{\sqrt{N}}\exp\left(-j\frac{2\pi}{N}(r-m)(s-m)\right), \quad 0 \le r,s \le N-1$$

with $m = (N-1)/2$. As was shown in [3], for the matrix $\mathbf{T}$ to commute with either version of the DFT, the matrix $\mathbf{Q}^2$ needs to be $\mathbf{W}^2$-centro-symmetric:

$$\mathbf{W}^2\mathbf{Q}^2\mathbf{W}^2 = \mathbf{Q}^2.$$

If we further require the commutator $\mathbf{C} = [\mathbf{Q},\mathbf{P}]$ to commute with the DFT, this implies that we require the matrix $\mathbf{Q}$ to be $\mathbf{W}^2$-anti-symmetric [3]:

$$\mathbf{W}^2\mathbf{Q}\mathbf{W}^2 = -\mathbf{Q}.$$

Here we specifically focus on the elements of the matrix $\mathbf{P}$:

$$\mathbf{P}_{rs} = \sum_{l=0}^{N-1}\sum_{m=0}^{N-1}\mathbf{W}_{rl}\mathbf{Q}_{lm}\mathbf{W}^*_{ms} \qquad (4)$$

Substituting the diagonal form of $\mathbf{Q}$ into this expression yields:

$$\mathbf{P}_{rs} = \sqrt{\frac{2\pi}{N}}\sum_{l=0}^{N-1}(l-m)\exp\left(-j\frac{2\pi}{N}(l-m)(r-s)\right). \qquad (5)$$

Specifically the matrix $\mathbf{Q}$ is non-diagonal, is purely imaginary because its elements are the DFT of an odd function. The matrix $\mathbf{Q}$ is also Toeplitz since the matrix elements depend only on $(r-s)$. In a similar fashion, we can evaluate the matrix elements of the commuting matrix $\mathbf{T}$ via:

$$\mathbf{T}_{rs} = \frac{2\pi}{N}\begin{cases}\displaystyle\sum_{l=0}^{N-1}(l-m)^2\exp\left(-j\frac{2\pi}{N}(l-m)(r-s)\right) & r \neq s \\ \displaystyle(r-m)^2 + \sum_{l=0}^{N-1}(l-m)^2 & r = s\end{cases}$$

The following symmetries can be inferred from the matrix elements:

1. for the diagonal form of the $\mathbf{Q}$ matrix and either form of the DFT, either the centered or the regular, the underlying commuting matrix has almost-Toeplitz symmetry.
2. Only main diagonal elements are different and follow a square law in accordance with the $(r-m)^2$ or the $(r-m-1)^2$ terms. Non-Toeplitz behavior of the commuting matrix is a consequence of non-Toeplitz[1] behavior of the matrix $\mathbf{Q}$.
3. The commuting matrix will also have $\mathbf{J}$-symmetry about $r = m$ along the diagonal for the centered DFT and $\mathbf{W}^2$-symmetry about $r = m+1$ along the diagonal for the DFT.
4. The commuting matrix is further positive semi-definite:
$$\mathbf{x}^H\mathbf{T}\mathbf{x} = \mathbf{x}^H(\mathbf{P}^H\mathbf{P} + \mathbf{Q}^H\mathbf{Q})\mathbf{x} = ||\mathbf{P}\mathbf{x}||_2^2 + ||\mathbf{Q}\mathbf{x}||_2^2 \ge 0$$

This motivates the equivalence of the commuting matrix $\mathbf{T}$ to the auto-correlation matrix of a weakly non-stationary time-series with elements:

$$\begin{matrix}\frac{2\pi}{N}\displaystyle\sum_{l=0}^{N-1}(l-m-1)^2\exp\left(-j\frac{2\pi}{N}(l-m)(r-s)\right) & r \neq s \\ \frac{2\pi}{N}(r-m-1)^2 + \frac{2\pi}{N}\displaystyle\sum_{l=0}^{N-1}(l-m-1)^2 & r = s\end{matrix}.$$

[1]A Toeplitz operator will produce a purely stationary basis of eigenvectors comprised of cosines and sines.

This weakly non-stationary time-series, autocorrelation viewpoint, exposes the aliasing in the almost-Toeplitz framework, since the quadratic power spectral term is not band-limited. The conclusion derived from this viewpoint is that the QMFD discretization of the non-bandlimited G-H operator will result in distortion that manifests as aliasing in the eigenvectors and a deviation from the linear eigenvalue spectrum of the G-H operator.

The time-series viewpoint also explicitly describes the windowing effects on the elements of the quasi-Toeplitz commuting matrix. Specifically the elements of the $\mathbf{Q}^2$ matrix are windowed with a rectangular window of duration N samples:

$$\mathbf{Q}_w^2 = \mathbf{\Lambda}_w \mathbf{Q}^2, \tag{6}$$

where $\mathbf{\Lambda}_w$ is a diagonal matrix with the window samples along the diagonal. By an appropriate choice of the window, we can affect the eigenvalue spectrum of the commuting matrix as depicted in Fig. (1), where we use a Kaiser window of duration $N = 256$ and parameter $\beta = 1.2$. The Kaiser window is chosen due to the degree of freedom that the parameter β affords in main lobe to side lobe trade-off. This has the effect of smoothing the fluctuations in the eigenvalue spectrum at the tail end as evident from Fig. 2 and expanding the region of the invertibility of the peak to parameter mapping [8]. To further reduce the distortions resulting from the truncation of the eigenvalue sequence of the G-H operator we now consider the case of the non-diagonal $\mathbf{Q}$, where we force the DFT commuting matrix to possess a linear eigenvalue spectrum.

4. QMFD APPROACH: NON-DIAGONAL Q CASE

As described in [7], the QMFD method needs to be modified so that the equations of motion are satisfied in the centered-DFT or regular-DFT basis. This is based on the observation that the $\mathbf{Q}$ and $\mathbf{P}$ tridiagonal basis corresponds to a diagonal number operator and a diagonal DFT operator. To obtain the number operator in the centered DFT basis or the regular DFT basis we similarity transform via the eigenvectors of the DFT or the CDFT obtained from the previous section. Specifically the $\mathbf{Q}$ and $\mathbf{P}$ tridiagonal matrices in the N-diagonal basis or the DFT diagonal basis are:

$$\mathbf{Q}_o = \frac{1}{\sqrt{2}} \begin{pmatrix} 0 & 1 & 0 & 0 & \dots \\ 1 & 0 & \sqrt{2} & 0 & \dots \\ 0 & \sqrt{2} & 0 & \sqrt{3} & \dots \\ 0 & 0 & \sqrt{3} & 0 & \sqrt{4}\dots \\ \vdots & \vdots & \vdots & \vdots & \dots \end{pmatrix}$$

$$\mathbf{P}_o = \frac{j}{\sqrt{2}} \begin{pmatrix} 0 & 1 & 0 & 0 & \dots \\ -1 & 0 & \sqrt{2} & 0 & \dots \\ 0 & -\sqrt{2} & 0 & \sqrt{3} & \dots \\ 0 & 0 & -\sqrt{3} & 0 & \sqrt{4}\dots \\ \vdots & \vdots & \vdots & \vdots & \dots \end{pmatrix}$$

The number operator in this tridiagonal representation is just the diagonal matrix:

$$\mathbf{N}_o = \mathrm{diag}(1, 3, 5, 7, \dots, 2N-1) \tag{7}$$

These quantities in the DFT basis are obtained via similarity transformation using the DFT eigenvectors $\mathbf{V}$ obtained from the previous section:

$$\mathbf{Q}_{\mathrm{new}} = \mathbf{V}\mathbf{Q}_o\mathbf{V}^H \text{ and } \mathbf{P}_{\mathrm{new}} = \mathbf{V}\mathbf{P}_o\mathbf{V}^H \tag{8}$$

The corresponding number operator in the DFT basis is:

$$\mathbf{T} = \mathbf{P}_{\mathrm{new}}^H\mathbf{P}_{\mathrm{new}} + \mathbf{Q}_{\mathrm{new}}^H\mathbf{Q}_{\mathrm{new}} = \mathbf{P}_{\mathrm{new}}^2 + \mathbf{Q}_{\mathrm{new}}^2 = \mathbf{V}\mathbf{N}_o\mathbf{V}^H, \tag{9}$$

where $\mathbf{V}$ are the orthogonal or unitary DFT eigenvectors obtained via the previous section with the almost-Toeplitz number operator. This transformed number operator by construction has a odd integer eigenvalue spectrum, and its eigenvectors are the DFT eigenvectors. This matrix therefore commutes with the appropriate DFT:

$$\mathbf{TW} = \mathbf{WT} \text{ or } [\mathbf{W}, \mathbf{T}] = \mathbf{0}.$$

The transformed number operator is however, not almost-Toeplitz as in the previous section but a $\mathbf{W}^2$-symmetric matrix corresponding to a non-diagonal $\mathbf{Q}_{\mathrm{new}}$ matrix:

$$\mathbf{W}^2\mathbf{T}\mathbf{W}^2 = \mathbf{T}\mathbf{W}^4 = \mathbf{T},$$

where we have used the observation that $[\mathbf{W}, \mathbf{T}] = \mathbf{0}$. Since the new number operator was constructed from the eigenvectors from the previous almost-Toeplitz framework, they carry with them the distortion due to truncation and aliasing. However, the distortion is reduced, in that the eigenvalue spectrum is closer to that of the G-H operator than what was obtained in the previous framework, thereby reducing one of the sources of distortion discussed in the introduction section. The characteristic feature of this approach is that we are specifying the eigenvalue sequence of the commuting matrix to be the truncated odd numbered spectrum. We can further reduce the effects of windowing of the eigenvalue sequence by choosing the window so that the eigenvalue sequence is:

$$\lambda_w[k] = (2k+1)w[k], \; 0 \le k \le N-1,$$

where $w[k]$ is an appropriately chosen window [1] that minimizes the effects of eigenvalue truncation. Figure 3 compares the peak to parameter mapping underlying both the diagonal $\mathbf{Q}$ approach and the non-Toeplitz framework for $N = 256$ using the Kaiser window. The mapping depicts a slight improvement in terms of invertibility of the mapping from 84.55 percent to 85.33 percent. This improvement is attributable to the fact that the eigenvalue spectrum in the non-diagonal $\mathbf{Q}$ case accommodates the effects of eigenvalue truncation. Figure 4(a) depicts the DFRFT spectra for a chirp signal for different values of the Kaiser window parameter β. For $\beta = 15$ with the non-diagonal $\mathbf{Q}$ formulation, we observe that there is significant distortion of the peaks arising from truncation. As can be observed specific values of the β parameter result in steeper slopes on the peaks of the underlying DFRFT spectrum. From Figure 4(b,c) we observe that the slopes of the spectral peaks are much steeper for $\beta = 1.2$ than for $\beta = 0.001$. Figure 4(d) depicts the eigenvalue spectrum corresponding to the different values of the Kaiser window parameter.

Figure 5(a) depicts the percentage invertibility associated with the $\mathbf{Q}$-windowing approach, the eigenvalue windowing approach, and the joint windowing approach using a Kaiser window with parameter $\beta = 1.2$. As can be observed, the joint windowing approach improves the invertibility of the peak to parameter mapping in relation to the other options. Furthermore, the improvement offered by the windowing approach is more significant for smaller transform sizes N, due to fact that the distortion due to truncation effects is more significant for these smaller values for N, where the invertibility approaches 91 % for larger matrix sizes N. Invertibility of the mapping as pointed out in [8] impacts the MSE of the corresponding chirp parameter estimates.

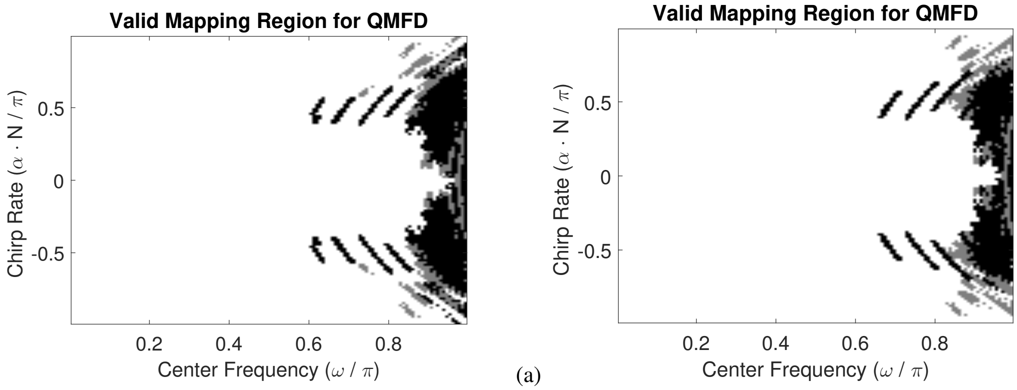

Fig. 2. Peak to parameter mappings for $N = 256$: (a) quasi-Toeplitz framework, and (b) non-diagonal $\mathbf{Q}$ formulation for the minimum-norm approach. The invertibility percentage of the mappings corresponding to the two operators are 84.55 percent and 85.33 percent respectively. The continued presence of a non invertible region in the mapping is a consequence of the truncation and aliasing distortion discussed in the introduction.

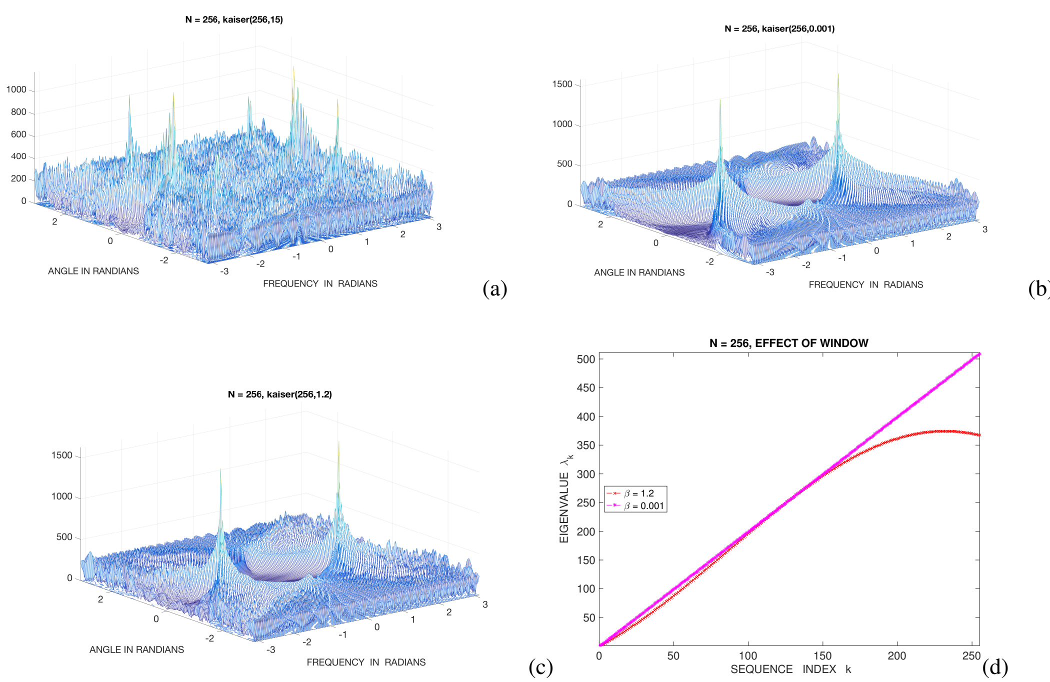

Fig. 3. Effect of windowing eigenvalue sequence: (a) DFRFT spectrum magnitude for Kaiser window with $N = 256,\ \beta = 15$, (b) DFRFT spectrum magnitude for Kaiser window with $N = 256,\ \beta = 0.001$, (c) DFRFT spectral magnitude for $\beta = 1.2$, and (d) eigenvalue spectrum with different Kaiser window parameters. Note that we obtain steeper slopes on the peaks of the DFRFT magnitude spectrum for $\beta = 1.2$ and for $\beta = 15$ we observe a significant amount of aliasing.

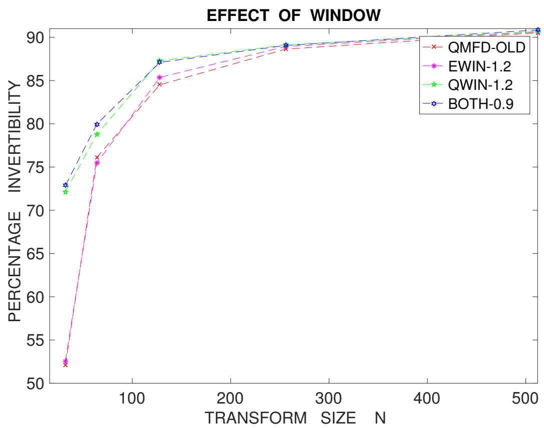

Fig. 4. Invertibility improvement: percentage of invertible pixels in the peak to parameter mapping for **Q**-windowing alone, with a Kaiser window with parameter $\beta = 1.2$, for eigenvalue windowing alone, using a Kaiser window with $\beta = 1.2$, and combined windowing using a Kaiser window with parameter $\beta_{1,2} = 0.9$

5. CONCLUSION

In this paper, we studied the problem of discretizing the Gauss-Hermite operator and the two basic sources of distortion: (a) eigenvalue truncation resulting in spectral distortion of the eigenvalue sequence, and (b) sampling of the eigenfunctions resulting in eigenvector aliasing. We studied two classes of matrices that commute with either the centered DFT or the regular DFT in the context of the QMFD method developed in [3] in terms of the distortion introduced in the transition from the continuous to the discrete FRFT.

We first studied the quasi-Toeplitz framework where the corresponding **Q** matrix is diagonal and developed a weakly non-stationary time-series viewpoint to expose distortion due to discretization in the approach. Means to minimize this distortion, such as windowing of the diagonal **Q** matrix with an appropriately chosen window function were studied. We then incorporated eigenvalue windowing into the more general approach to mitigate truncation effects at the end of the eigenvalue spectrum. A Kaiser windowed version of the truncated odd integer eigenvalue spectrum, resulted in sharper peaks in the underlying DFRFT spectra in comparison to the boxcar windowed spectra and eventually translated to a wider invertibility region for the peak to parameter mappings. Improvement from windowing is specifically more pronounced for smaller matrix sizes, where the distortion from discretization is more pronounced.

6. REFERENCES

[1] F. J. Harris, "On the Use of Windows for Harmonic Analysis with the Discrete Fourier Transform," *Proc. of IEEE*, Vol. 66, pp. 51-83, 1978.

[2] L. B. Alameida, "The Fractional Fourier Transform and Time-Frequency Representations," *IEEE Trans. Sig. Process.*, Vol. 42, No. 11, pp. 3084-3091, 1994.

[3] Balu Santhanam and T. S. Santhanam, "On Discrete Gauss-Hermite Functions and Eigenvectors of the Discrete Fourier Transform," *Signal Processing*, Vol. 88, No. 6, pp. 2738 - 2746, November 2008.

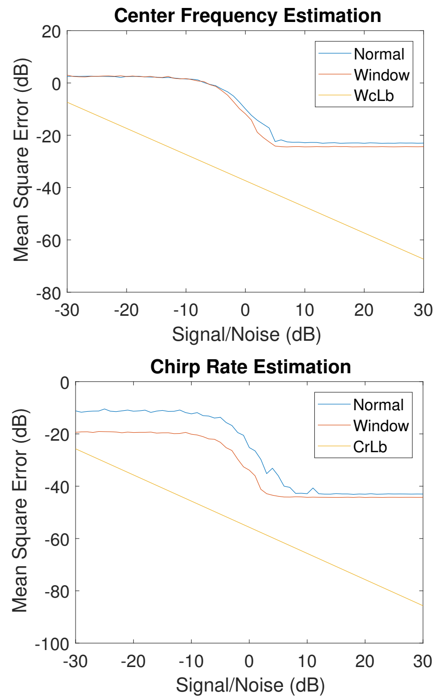

(a)

(b)

Fig. 5. (a,b) Impact of windowing on the MSE of parameter estimates from the minimum-norm algorithm, depicting improved invertibility of the underlying peak to parameter mapping with combined **Q**-matrix and eigenvalue windowing.

[4] B. Dickinson and K. Steiglitz, "Eigenvectors and Functions of the Discrete Fourier Transform," *IEEE Trans. Sig. Process.*, Vol. 30, No. 1, pp. 25 - 31, February 1982.

[5] F. Grunbaum, "The eigenvectors of the Discrete Fourier transform: A version of the Hermite functions," *Journal of Mathematical Analysis and Applications*, Vol. 88, No. 2, pp. 355 - 363, August 1982.

[6] S. Clary and D. Mugler, "Shifted Fourier Matrices and their Tridiagonal Commutors," *SIAM Journal Matrix Analysis and Applications*, Vol. 24, No. 3, pp. 809 - 821, January 2003.

[7] Thalanayar Santhanam and Balu Santhanam, "The Discrete Fourier Transform and the Quantum Mechanical Oscillator in a Finite-Dimensional Hilbert Space," *Journal Of Physcis A: Theoretical*, Vol. 42, pp. 205303, May 2009.

[8] Ishwor Bhatta and Balu Santhanam, " A Comparative Study Of Commuting Matrix Approaches For The Discrete Fractional Fourier Transform," *Proc. of IEEE Signal Processing and SP Education Workshop*, pp. 103-108, 2015.

[9] Q. Wang, M. Pepin, R. J. Beach, R. Dunkel, T. Atwood, B. Santhanam, W. Gerstle, A. W. Doerry, and M. M. Hayat, "SAR-based Vibration Estimation using the Discrete Fractional Fourier Transform," *IEEE Trans. Geoscience and Remote Sensing*, Vol. 50, No. 10, pp. 4145-4156, 2012.

[10] Q. Wang, M. Pepin, A. Wright, R. Dunkel, T. Atwood, B. Santhanam, W. Gerstle, A. W. Doerry, and M. Hayat, " Reduction of Vibration-Induced Artifacts in Synthetic Aperture Radar Imagery, " *IEEE Trans. Geoscience and Remote Sensing*, Vol. 52, No. 6, pp. 3063-3073, 2014.